Journal of Controlled Release 235 (2016) 72–81

Contents lists available at ScienceDirect

Journal of Controlled Release

journal homepage: www.elsevier.com/locate/jconrel

Non-invasive, neuron-specific gene therapy by focused ultrasound-induced blood-brain barrier opening in Parkinson's disease mouse model

Chung-Yin Lin [a,b,**], Han-Yi Hsieh [c], Chiung-Mei Chen [d], Shang-Rung Wu [e], Chih-Hung Tsai [c], Chiung-Yin Huang [f], Mu-Yi Hua [g], Kuo-Chen Wei [f], Chih-Kuang Yeh [h], Hao-Li Liu [a,c,*]

[a] Medical Imaging Research Center, Institute for Radiological Research, Chang Gung University/Chang Gung Memorial Hospital, Taoyuan 333, Taiwan
[b] Department of Nephrology, Division of Clinical Toxicology, Chang Gung Memorial Hospital, Lin-Kou Medical Center, Taoyuan 333, Taiwan
[c] Department of Electrical Engineering, Chang Gung University, Taoyuan 333, Taiwan
[d] Department of Neurology, Chang Gung Memorial Hospital, Taoyuan 333, Taiwan
[e] Institute of Oral Medicine, National Cheng Kung University, Tainan 701, Taiwan
[f] Department of Neurosurgery, Chang Gung Memorial Hospital, Linkou Medical Center and College of Medicine, Chang Gung University, Taoyuan 333, Taiwan
[g] Department of Chemical and Material Sciences, Chang Gung University, Taoyuan 333, Taiwan
[h] Department of Biomedical Engineering and Environmental Sciences, National Tsing Hua University, Hsinchu 300, Taiwan

ARTICLE INFO

Article history:
Received 29 February 2016
Received in revised form 28 April 2016
Accepted 24 May 2016
Available online 26 May 2016

Keywords:
Focused ultrasound
Gene therapy
Blood-brain barrier opening
Microbubbles
GDNF

ABSTRACT

Focused ultrasound (FUS)-induced with microbubbles (MBs) is a promising technique for noninvasive opening of the blood-brain barrier (BBB) to allow targeted delivery of therapeutic substances into the brain and thus the noninvasive delivery of gene vectors for CNS treatment. We have previously demonstrated that a separated gene-carrying liposome and MBs administration plus FUS exposure can deliver genes into the brain, with the successful expression of the reporter gene and glial cell line-derived neurotrophic factor (GDNF) gene. In this study, we further modify the delivery system by conjugating gene-carrying liposomes with MBs to improve the GDNF gene-delivery efficiency, and to verify the possibility of using this system to perform treatment in the 1-Methyl-4-phenyl-1,2,3,6-tetrahydropyridine (MPTP)-induced animal disease model. FUS-BBB opening was verified by contrast-enhanced MRI, and GFP gene expression was verified via in vivo imaging system (IVIS). Western blots as well as enzyme-linked immunosorbent assay (ELISA) were conducted to measure protein expression, and immunohistochemistry (IHC) was conducted to test the Tyrosine hydroxylase (TH)-neuron distribution. Dopamine (DA) and its metabolites as well as dopamine active transporter (DAT) were quantitatively analyzed to show dopaminergic neuronal dopamine secretion/activity/metabolism. Motor performance was evaluated by rotarod test weekly. Results demonstrated that the LpDNA-MBs (gene-liposome-MBs) complexes successfully serve as gene carrier and BBB-opening catalyst, and outperformed the separated LpDNA/MBs administration both in terms of gene delivery and expression. TH-positive IHC and measurement of DA and its metabolites DOPAC and HVA confirmed improved neuronal function, and the proposed system also provided the best neuroprotective effect to retard the progression of motor-related behavioral abnormalities. Immunoblotting and histological staining further confirmed the expression of reporter genes in neuronal cells. This study suggests that FUS exposures with the administration of LpDNA-MBs complexes synergistically can serve as an effective gene therapy strategy for MPTP-animal treatment, and may have potential for further application to perform gene therapy for neurodegenerative disease.

1. Introduction

Parkinson's disease (PD) is the second most common neurodegenerative disorder worldwide, affecting 1% of the elderly population with a higher prevalence [1]. Patients typically develop progressive loss of the nigro-striatal dopaminergic neurons and eventually resulting in wide-spread neuronal cell death [2,3]. Currently no definite treatment approach exists to slow the progression of neurodegenerative disease. Patients suffer a loss of movement controlling and other such

* Correspondence to: H.L. Liu, Department of Electrical Engineering, Chang Gung University, Taoyuan 333, Taiwan.
** Correspondence to: C.Y. Lin, Medical Imaging Research Center, Chang Gung University, Taoyuan 333, Taiwan.
E-mail addresses: winwood5782@gmail.com (C.-Y. Lin), haoliliu@mail.cgu.edu.tw (H.-L. Liu).

http://dx.doi.org/10.1016/j.jconrel.2016.05.052
0168-3659/

symptoms, mainly due to degeneration of dopaminergic neurons in the substantia nigra (SN), coupled with a depletion of dopamine (DA) and metabolites in the nigrostriatal projections [4,5].

Gene therapy is a therapeutic approach that aims to treat disease by genetically modifying neuronal cells to relieve relevant-symptoms or even reverse PD progression [6,7]. For example, glial cell line-derived neurotrophic factor (GDNF) is a potent agent for PD therapy due to its neuroprotective and neurotrophic effects [8,9]. The overexpression of neuroprotective genes to promote regeneration of DA in activated neurons offers potentially significant symptoms alleviation while slowing disease progression [10]. This strategy allows for treatment using putative neuroprotective-agents prior to significant/irreversible neuronal loss [11]. However, one of the major challenge to this approach is the blood-brain barrier (BBB), in which tight junctions between the endothelial cells block the penetration of molecules >400 Da, thus preventing CNS uptake therapeutic drugs/genes [12]. In addition, therapeutic genes administered intravenously are rapidly degraded through reticuloendothelial system (RES) uptake and clearance, thus typically requiring the invasive intracranial local injection of therapeutic genes [13,14].

Transcranial focused ultrasound exposure with microbubbles (MBs) can temporally and locally open the BBB to allow large therapeutic substances to penetrate the targeted CNS regions [15–18] in various species ranging from small to larger animal [19–21]. Regarding gene-vector delivery, we have previously shown that the technique can be synergistically combined with a liposome-containing plasmid DNA (LpDNA) system to significantly promote GDNF transfection (5–10 fold increase in GDNF measures as compared to controls) at target CNS sites in normal animals [22]. It is reasonable to surmise that GDNF gene delivery and expression in SN via LpDNA system combined with FUS-BBB opening should be beneficial to PD progression control, since previous studies have confirmed that supplemental GDNF supplement can help prevent neuronal death and can retard PD progression [23,24]. In addition, FUS-induced BBB opening relies on the administration of MBs to provide cavitation-induced sheer stress/radiation force in capillaries to trigger tight-junction opening. A more efficient design involves forming LpDNA-MBs complex [25,26] to maximize gene-vector delivery into the brain since the MB-generated force directly radiates LpDNA toward tight-junctional crafts. Therefore, we hypothesize that the LpDNA-MBs complex with an FUS-induced BBB opening can effectively deliver genes to the brain to provide effective PD treatment.

The study develops and evaluates the efficacy of a CNS gene delivery system via the synergistic use of FUS-induced BBB opening with the GDNF-gene-vector/MBs complex to perform noninvasive GDNF gene delivery and evaluate its treatment efficacy in 1-methyl-4-phenyl-1,2,3,6-tetrahydropyridine (MPTP) mouse model of PD. We propose a novel GDNF-gene-vector/MBs complex design by synthesizing biotinylated liposome-containing pDNA (LpDNA) to bind avidin-MBs via biotin-avidin linkages. Once in the cell, the LpDNA eventually enters the nucleus and enhances the protein expression. The designed LpDNA contains green fluorescence protein (GFP) genes and GDNF genes to allow for in vivo detection of gene expression. Fig. 1 shows the proposed FUS gene delivery system. Biophysical/biochemical analysis was conducted to characterize the LpDNA-MBs complex system. We measured the expression levels of proteins and metabolites, conducted pathological examinations, assessed motor performance of MPTP-treated mice, and compared the proposed LpDNA-MBs complex system with separated LpDNA/MBs administration. We also present immunohistochemistry (IHC) staining evidence that neuronal cells are the major target to be transduced via the proposed system.

2. Material and methods

2.1. Plasmid DNA (pDNA) preparation

A single bacterial colony containing a plasmid encoding both the GFP gene (marker gene) and the glia-derived neurotrophic factor (GDNF) gene (therapeutic gene) was cultured and inoculated in 500 mL LB medium. The mixture was then incubated for about 24 h at 37 °C with shaking at 300 rpm. The bacteria cells were harvested by centrifugation at 3000 ×*g* for 30 min at 4 °C. Following to the manufacturer's instructions, the samples were centrifuged at 15,000 ×*g* for 10 min and the supernatant was decanted. Then, 200 μL of double-distilled autoclaved water (DDAC) was added to the pellet, followed by 20 μL of sodium acetate along with 550 μL of cold ethanol. The mixture was centrifuged at 4 °C for about 15 min. Finally the supernatant was gently removed and

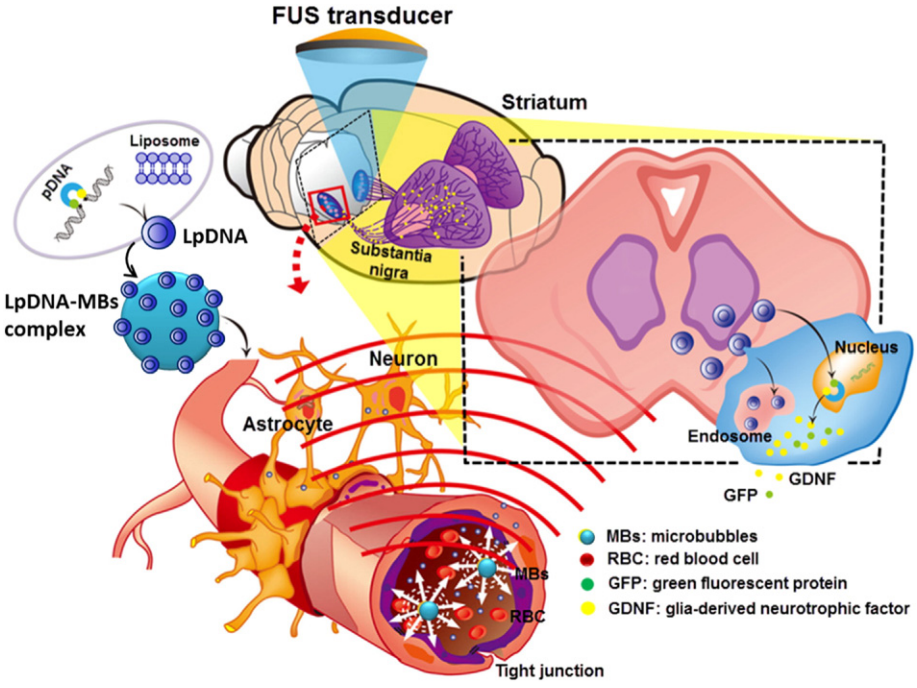

Fig. 1. Schematic representation of the synergistic use of the LpDNA-MBs complex to assist FUS-induced BBB opening to perform noninvasive and targeted GDNF gene delivery for MPTP-treated animals. FUS = focused ultrasound; BBB = blood-brain barrier.

100 μL of DDAC water was added to the plasmid. The plasmid concentration was taken using a Nanodrop (ND-1000, Thermo Fisher Scientific Inc. Waltham, MA) at wavelengths of 260- and 280-nm. A ratio greater than 1.8 indicated that the purified pDNA was free of contaminants.

2.2. Biotinylated liposome-containing plasmid DNA (LpDNA) formation

Biotinylated liposomes containing dipalmitoylphosphatidylcholine (DPPC), cholesterol (Chol), 1,2-distearoyl-*sn*-glycero-3-phosphoethanolamine-*N*-[biotinyl(polyethylene glycol)2000] (DSPE-PEG (2000)-Biotin) (Avanti Polar Lipids Inc., Alabaster, AL), and α-tocopherol in a 3:1:1:0.004 M ratio were made using the film hydration method as previously described [27]. Briefly, the lipid mixture dissolved in chloroform was dried in a flask to produce a homogeneous lipid film. The film was then hydrated with a suspension of condensed plasmid DNA (pDNA) at 42 °C until the film dispersed from the bottom of the flask. The suspension was then sonicated and extruded 10 times through 200-nm polycarbonate filters using an Avanti Mini Extruder (Alabaster, AL), and then passed through a spin column to remove the unencapsulated pDNA. After centrifugation at 16,100 ×*g* for 15 min and supernatant collection, the concentration of LpDNA in the liposomes was determined spectrophotometrically by measuring at a wavelength of 260 nm (Hitachi F-7000, Tokyo, Japan) following the method used in our previous study [22].

2.3. LpDNA-microbubble complex preparation

The LpDNA solution in PBS and avidinylated MBs (Targeson Inc., San Diego, CA) were mixed at a 1:1 volume ratio and stirred for 1 h at room temperature. The avidinylated MBs were gently stirred in the LpDNA liquid to form the LpDNA-conjugated avidinylated MBs (LpDNA-MBs). The mixture was spun for 10 min at 20 ×*g* using a fixed rotor centrifuge (Eppendorf 5415C, Hauppauge, NY). The higher density of the LpDNA-MBs caused them to settle at the bottom, while untargeted MBs remained in the top layer. We discarded the top layer, and re-suspended the targeted MBs in a total volume of 1.0 mL of PBS. Encapsulation efficiency was calculated as the fraction of original pDNA incorporated into the LpDNA vesicles. The mean particle size and zeta potential of pDNA, LpDNA, avidinylated MBs, and LpDNA-MBs were respectively measured by dynamic light-scattering (DLS) and zeta potential on a Nano-ZS90 particle analyzer (Malvern Instruments, Malvern, Worcestershire, UK). An average of 10 runs was completed, with each run requiring about 3 min. The avidinylated MBs and LpDNA-MBs were prepared and imaged by cryogenic-transmission electron microscopy (Cryo-TEM). Particle number concentrations were calculated from the masses of LpDNA and LpDNA-MBs suspended in a 1:100 (*v*/*v*) ratio in a cuvette with DDAC water by Mastersizer™ 2000 (Malvern Instruments, Malvern, Worcestershire, UK). The measured concentration was generated using the Mastersizer analysis software and reported in the form of a population percentage.

2.4. PD animal model

Eight-week-old Balb/c male mice, each weighing about 25 g, were used for all experiments. To implement a mouse model of PD using the neurotoxin MPTP, nigrostriatal changes caused a loss of striatal dopamine, as in previous studies [28]. Six test groups of mice (n = 15 per group) received the intraperitoneal injection of MPTP-HCl (40 mg/kg; Aldrich-Sigma, St. Louis, MO) in saline once a day, 5 days per week for 3-weeks, and were killed at 8 days after the last injection. Control mice received saline only. All experiments met the criteria outlined by the Institutional Animal Care and Use Committee of Chang Gung University (CGU-IACUC), and were performed according to the guidelines in *The Handbook of the Laboratory Animal Center*, Chang Gung University.

2.5. Focused ultrasound exposure setup

A single-element FUS transducer (Imasonics SAS, France; center frequency = 500 kHz, diameter = 64 mm, radius of curvature = 63.2 mm, electric-to-acoustic efficiency of 99%) was placed in an acrylic water tank filled with distilled and degassed water. The focus of the ultrasonic field was positioned on the desired region. The signals from the function generator (33120A, Agilent, Palo Alto, CA) were boosted with a power amplifier (150A100B, Amplifier Research, Souderton, PA), measured using an inline power meter (Model 4421, Bird Electronics Corp., Cleveland, OH), and then used to drive the FUS transducer. The animal was placed directly under a 4 × 4 cm^2 window of thin polymer film at the bottom of the acrylic tank, in acoustic connection using acoustic transmission gel (Pharmaceutical Innovations, Newark, NJ). The output acoustic pressure was calibrated using a calibrated polyvinylidene-difluoride-type (PVDF) hydrophone (Model HNP-0400, ONDA, Sunnyvale, CA, USA). Microbubbles (MBs) or LpDNA-MBs complexes with a concentration of 5 × 10^8 MBs/mL were administered intravenously prior to FUS exposure. Input electric power ranging from 0.8–5.4 W was used (equivalent to negative pressure 0.3–0.8 MPa). Following to our previous in vivo study, the experiment used burst-mode ultrasound with a burst length of 10 ms, a pulse-repetition frequency (PRF) of 1 Hz, and an exposure duration of 60 s.

2.6. Imaging assessment using in vivo imaging system (IVIS) and MRI

Induction of FUS-induced BBB opening was verified via magnetic resonance imaging (MRI) and evens blue (EB) extravasation. A 7-Tesla magnetic resonance scanner (Bruker ClinScan, Germany) was used to acquire a 4-channel surface coil for monitoring. Anatomical images were scanned before and after FUS sonication by performing a gradient echo FLASH sequence to acquire T1W1 images with the following imaging parameters: pulse repetition time (TR) / echo time (TE) = 230 ms; FOV = 30 × 17.82 mm^2; in-plane resolution = 256 × 256 pixels; slice thickness = 0.8 mm; flip angle = 70°. Following sonication, an intravenous bolus (0.1 mmol/kg) of gadopentetate dimeglumine (Gd-DTPA) MRI contrast agent (Magnevist, Berlex Laboratories, Wayne, NJ) was administered to determine the BBB opening. To stain the BBB-opened brain areas, Evens blue (EB) at 30 mg/kg was injected immediately after the mice were exposed to FUS sonications. The mice were sacrificed approximately 2 h after EB injection. HE staining was used to assess the resulting histological damage at both contralateral and ipsilateral SN.

In addition, the activity and location of gene delivery were identified at 24 and 48 h after FUS treatment via the bioluminescence imaging (IVIS-200, Xenogen Corporation, CA). The signal intensity of the acquired frames was quantified by Living Image 2.5 software (Caliper Life Sciences, MA) to assess transgene expression activity.

2.7. Animals study procedure and design

To study the effect of transgenic induction on the neuroprotective response in the FUS-BBB opening in the contralateral and ipsilateral SN area, four experimental groups were composed: LpDNA (pDNA at 27 μg), FUS exposure only (no LpDNA, no avidinylated MBs), LpDNA (pDNA at 27 μg) injection followed by avidinylated MBs injection with FUS exposure, and LpDNA-MBs (27 μg of pDNA at LpDNA-conjugated avidinylated MBs) with FUS exposure. The experiment for each group was run twice a week for 3-weeks. If not otherwise specified, the LpDNA was injected intravenously through the tail vein. The avidinylated MBs or the LpDNA-MBs were injected and FUS exposure was immediately applied to the brains to open the BBB, resulting in enhanced delivery of LpDNA across the BBB. In addition, the FUS exposures were followed about 2 min later by an additional FUS sonication at the ipsilateral hemisphere. We applied pulsed FUS sonication with a 10-ms burst length, a 1% duty cycle, a 1-Hz pulse repetition frequency

(RPF), and a 60 s insonation duration at the contralateral hemisphere, and a further 30 s insonation at the ipsilateral hemisphere. The LpDNA-MBs (mean diameter of about 1.5 μm, and MB concentration of 5×10^8 bubbles/mL) were intravenously injected through the tail vein at a dose of 4 μL/kg.

Tests were conducted on six animal groups: (a) normal control; (b) MPTP-treated only; (c) MPTP-treated with LpDNA administration; (d) MPTP-treated with FUS exposure; (e) MPTP-treated with separate LpDNA/MBs administrations following FUS exposure; and (f) MPTP-treated with LpDNA-MBs administration following FUS exposure. Induction of mice with 40 mg/kg MPTP for 3-weeks resulted in about 60% loss of TH-positive neurons. Fig. 2 shows the detailed time course for the MPTP-treated PD-model mice, with their treatment timepoints, scheduled rotarod, and histological analysis with or without FUS sonication in the presence of LpDNA or avidinylated MBs.

2.8. Motor-related behavioral test

PD is a neurodegenerative disorder with typical motor symptoms, and our experiment assessed animal motor performance using an accelerating rotarod apparatus. Repeated testing of adult PD-model mice and normal controls over a 4-week period revealed progressive impairments in motor learning skill and motor performance. Subject body weight and general health condition were monitored daily during the period of exposure to MPTP drugs or LpDNA or FUS treatment. No animal died during this period. All motor skill learning occurred during the light phase of the 12-h light/dark cycle. Motor coordination and balance were assessed using a rotarod apparatus (RT-01, Singa Technology Corp., Taiwan). The animal was placed on the rolling rod at an initial speed of 5 rpm. Five trials were run at 3 min intervals at accelerated speeds (5–30 rpm). Each group contained fifteen mice, and each mouse repeated the trial three times, recording the time until the subject fell off the rotarod.

2.9. Protein expression

The protein levels of GDNF and GFP expressed in the striatal tissues were respectively detected using the GDNF and GFP ELISA Immunoassay Kits (abcam®, Cambridge, MA) as per manufacturer's instructions. Absorbance of tissue lysates were separately measured at 450 nm and 488 nm for full strength, with 1:10, 1:100, 1:500, 1:1000, 1:5000 dilutions using a microplate ELISA Reader (Molecular Devices, LLC., Sunnyvale, CA). The resulting concentrations of GDNF and GFP proteins were adjusted according to the dilution folds and replicates were averaged to obtain their final concentration levels. The protein levels were normalized to express a normal control for the transfection efficiency in striatal tissues.

2.10. Neurochemical analysis

Levels of dopamine (DA), 3,4-dihydroxyphenylacetic acid (DOPAC), and homovanillic acid (HVA) were determined by HPLC using a modified methods described previously [29,30]. Briefly, the isolated brain striatum was homogenized in 500 μL of PRO-PREP™ protein extraction solution (iNtRON Biotechnology Inc., Summit, NJ). Samples were centrifuged at 10,000 × *g* for 30 min and then filtered through a 0.45 μm syringe membrane. DA, DOPAC, and HVA from the supernatant were analyzed by the HPLC system using a C18 column with a UV detector at 280 nm. The sample was passed through the HPLC system using a mobile phase of 89.5% 0.1 M of trichloroacetic acid, 10^{-2} M of sodium acetate, 10^{-4} M of ethylenediaminetetraacetic acid, and 10.5% methanol (pH 3.8) at a flow rate of 1.0 mL/min.

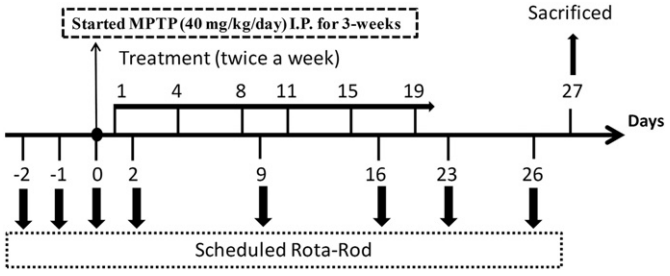

Fig. 2. Timeline of the study design and schematic of the mouse treatment-procedure sequences.

2.11. Western Blotting

Fresh frozen brain tissues from the SN and striatum (ST) were homogenized in PRO-PREP™ protein extraction solution, kept overnight, and then centrifuged at 10,000 × *g* for 30 min. After centrifugation to remove tissue debris, the protein contents of the tissue homogenates were determined according to the Bradford method [31]. The supernatant with 20 μg protein was dissolved in a sample buffer, separated by 10% SDS-PAGE, and then transferred to a polyvinylidene fluoride (PVDF) membrane. The PVDF membrane was further incubated with a primary rat anti-DAT antibody (abcam®, Cambridge, MA), rabbit anti-GFP antibody (R&D Sys., Minneapolis, MN) or mouse anti-GDNF antibody (OriGene Technologies, Inc., Rockvile, MD) at a 1:500 dilution and a secondary mouse anti-rat, donkey anti-rabbit and rabbit anti-mouse antibodies (Molecular Probes Inc., Grand Island, NY) at a 1:1000 dilution. To measure the optical density of the positive bands, the film was scanned using the BioSpectrum Imaging System (UVP LLC, Upland, CA).

2.12. Immunohistochemistry staining

To evaluate the effect of dopaminergic neurodegeneration caused by MPTP administration and treatment-procedure on the neuroprotective impairment, an immunohistological staining of Tyrosine hydroxylase (TH) was performed in brain SN sections from normal control and PD-model mice. Brain tissues were prepared and sectioned using standard procedures to examine neuronal morphology. For immunohistochemistry, a substantia nigra brain section was stained with anti-TH antibody (dilution 1:5000, Novus Biologicals, Littleton, CO) using the ABC-DAB method. Slide images were then recorded with a phase-contrast microscope (TissueFAX Plus, TissueGnostics, Austria). To identify the effect of therapeutic response on neuronal function, tissue sections were stained overnight at 4 °C with the following primary antibodies: anti-GFP (dilution 1:500, Abcam®, Cambridge, MA), anti-GDNF (dilution 1:500, OriGene Technologies, Inc., Rockvile, MD), and anti-MAP2 (dilution 1:1000, Santa Cruz Biotechnology, Inc., Dallas, TX). After rinsing in PBS, the sections were incubated in secondary antibody with goat anti-rabbit fluorescence 594 or donkey anti-mouse fluorescence 594 (1:1000, for GFP or MAP2) or with rabbit anti-mouse fluorescence 488 (1:1000, for GDNF) for 1 h at room temperature. After rinsing in PBS, coverslips were applied on slides with an anti-fade reagent with the nuclear marker DAPI (Molecular Probes Inc., Grand Island, NY). The sections were then imaged by a Leica TCS SP8X confocal microscope (Leica Microsystems, Wetzlar, Germany).

2.13. Statistical analysis

All are presented as mean ± standard deviation (SD). Statistical analysis was performed on a personal computer using SPSS version 16.0 (SPSS Inc., Chicago, IL) statistical software. Statistical differences were assessed using ANOVA with post-hoc Tukey test, Mann-Whitney *U* test, or Kolmogorov-Smirnov's test, where appropriate. Statistical significance was denoted as "*" when $p < 0.05$, "**" when $p < 0.01$, and "***" when $p < 0.005$.

3. Results

3.1. Characterization of LpDNA and LpDNA-microbubble complexes

The amount of encapsulated pDNA inside liposomes was calculated based on the absorbance of pDNA in the resulting LpDNA, with the measured LpDNA entrapment efficiency of 82.5%. The size distribution of LpDNA, avidinylated MBs, and LpDNA-MBs was 105–400 nm, 700–2150 nm, and 100–4200 nm, respectively (Fig. 3A). Zeta potential was measured to determine MBs-LpDNA conjugating affinity, and the measured potential distribution of pDNA, LpDNA, avidinylated MBs, and LpDNA-MBs were -19.2 ± 3.8, -19.1 ± 3.5, $+20.3 \pm 2.7$, and $+2.3 \pm 1.9$ mV, respectively. There was no electrical difference between the mean zeta potentials of pDNA/LpDNA when compared with a weakly positive charge of the biotinylated liposomes, implying that biotinylated liposomes allowed for DNA loading. Relatively minimal changes in surface charges were observed after the incubation of avidinylated MBs and LpDNA (-18 ΔmV), implying successful conjugation of the LpDNA and the MBs. The surface charges of the slightly positive liposomes increased slightly, suggesting a significantly greater binding capacity with negatively charged pDNA.

Fig. 3C and D respectively show Cryo-TEM images of avidinylated MBs and the LpDNA-MBs. The formation of LpDNA-MBs conjugation was confirmed by the presence of LpDNA (white arrows), whereas the LpDNA appeared to be absent in the claw-spheroid shaped structure. After adding avidinylated MBs to LpDNA, the mean size of the LpDNA-MBs was 1.5 μm with a polydisperity index of 0.72 (Fig. 3E). The LpDNA-MBs concentration was estimated to be as high as 5×10^8/mL.

3.2. FUS-induced blood-brain barrier (BBB) opening

Next, we evaluated the impact of FUS exposure on opening the BBB near the substantia nigra (SN) region. Fig. 4A shows a typical example of a contrast-enhanced MRI and the corresponding EB-dye stained brains to confirm BBB-opening efficacy via the proposed system. Enhanced T1-weighted images confirm the BBB-opening scale under various exposure pressure levels (Fig. 4A). Subtracted MR images showed no apparent signal intensity (SI) increase in the brain at 0.3-MPa exposure except in the ventricles, indicating the BBB was still intact. 0.5-MPa exposure induced apparent SI changes in the surrounding SN regions, whereas 0.8-MPa exposure induced a more profound SN BBB-opening effect and more apparent Gd-DTPA leakage. The observation of Gd-DTPA leakage was also confirmed by EB-stained brain sections, with 0.5- and 0.8-MPa both inducing EB leakage (the latter providing more profound leakage). HE staining of 0.8-MPa exposure also showed scattered erythrocytes extravasations, which may raise concerns for potential capillary/brain tissue damage, but this was not observed in the 0.5-MPa exposure. The 0.5-MPa exposure level was thus used for the following PD-animal treatments. In addition, the efficacy of targeted transfection was evaluated through IVIS (Fig. 4B). FUS-triggered LpDNA-MBs delivery resulted in a significant increase of GFP expression over LpDNA administration alone and control animals.

3.3. GFP and GDNF expression after FUS-BBB opening

Fig. 5 shows Western blotting analysis results for the GFP and GDNF protein expression. Using a normal control as baseline, FUS exposure with separate LpDNA/MBs administration or LpDNA-MBs complex both yield significantly increased GDNF and GFP protein expressions. This suggests that FUS exposure successfully opened the BBB, thus inducing LpDNA penetration and eventually transducing GDNF and GFP expression. In addition, both GDNF and GFP were highly expressed in the LpDNA-MBs complex approach with a protein expression level exceeding that of the separate LpDNA/MBs administration. This was consistent with the GDNF and GFP proteins levels analyzed by ELISA immunoassay shown in Fig. 6A and B (taking the normal GFP and GDNF control levels as baseline). This verifies that the LpDNA-MBs complex + FUS system can provide more effective gene delivery.

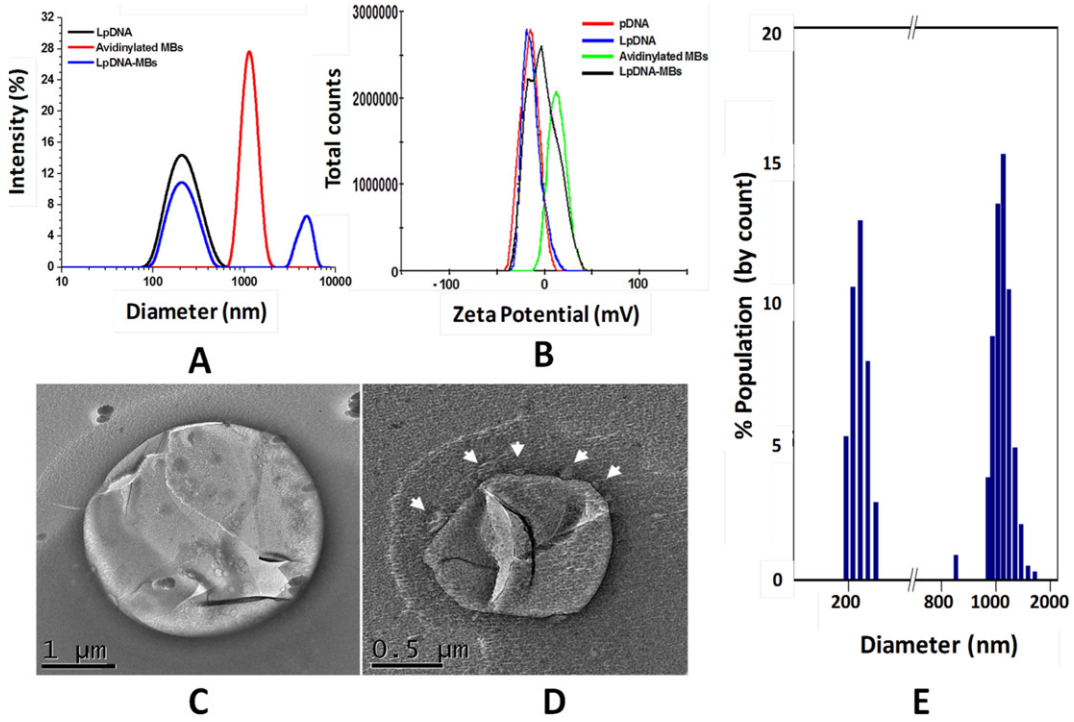

Fig. 3. Characterization of the LpDNA-MBs complexes. (A) Size distribution of LpDNA, avidinylated MBs, and LpDNA-MBs measured by dynamic light scattering. (B) Zeta potential of pDNA, LpDNA, avidinylated MBs, and LpDNA-MBs. (C, D) Cryo-TEM images of the avidinylated MBs and LpDNA-MBs complexes. (E) Size population percentage of LpDNA and LpDNA-MBs.

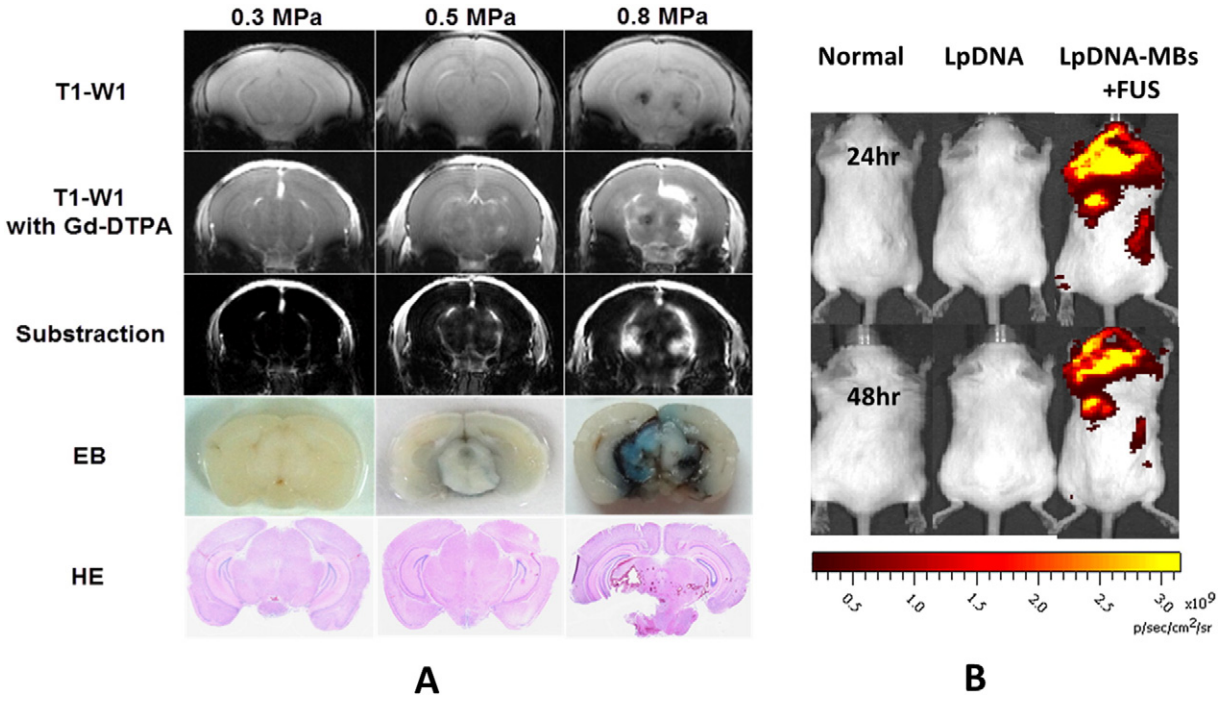

Fig. 4. (A) Representative contrast-enhanced T1-weighted MR images (1st row: before contrast injection, 2nd row: after contrast injection, 3rd row: subtracted images), corresponding EB-stained brain sections (4th row) and HE stained section (5th row) under various FUS exposure pressures. (B) In vivo bioluminescent imaging acquired at 24 and 48 h after LpDNA administration in sham control, LpDNA administration only, and LpDNA-MBs + FUS exposure.

3.4. The effects of neurochemical proteins expressed after FUS-BBB opening

To examine the GDNF protein expression and DA secretion, levels of DA and its key metabolites, 3,4-dihydroxyphenylacetic acid (DOPAC) and homovanillic acid (HVA) were also analyzed using HPLC (Fig. 6C, taking the normal control of DA, DOPAC, and HVA as baseline). MPTP-treated mice and MPTP-treated mice receiving LpDNA only or FUS exposure only showed a steep decrease in DA content in the striatum (ST) compared to the control mice, from 25.0 ± 8.2 μg/mL protein to 1.2 ± 0.3, 3.4 ± 0.8, 1.8 ± 0.6 μg/mL protein. Similarly, a DOPAC level decrease from 2.8 ± 1.3 μg/mL to 0.6 ± 0.2, 3.1 ± 1.3, 3.3 ± 0.8 μg/mL, and a slight decrease in HVA level from 37.5 ± 4.3 μg/mL to 22.1 ± 8.3, 36.7 ± 4.2, 30.8 ± 10.3 μg/mL, respectively. In contrast, MPTP-treated mice receiving the FUS-BBB opening with either separate LpDNA/MBs or LpDNA-MBs complex resulted similarly smaller decreases of DA compared to the control mice (14.8 ± 10.1 μg/mL and 18.9 ± 8.8 μg/mL vs 25.0 ± 8.2 μg/mL), DOPAC level (8.2 ± 3.6 μg/mL and 5.1 ± 0.6 μg/mL vs 2.8 ± 1.3 μg/mL), and HVA level (32.3 ± 15.6 μg/mL and 27.9 ± 2.6 μg/mL vs 37.5 ± 4.3 μg/mL) in ST than that found in the untreated or invalid-treated groups. The elevated levels of DOPAC and HVA in these two groups confirmed restoration of dopaminergic neuronal function in PD-model mice via FUS-BBB opening.

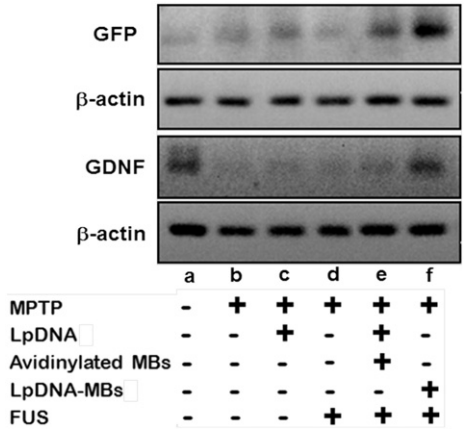

Fig. 5. Western blot to detect GFP and GDNF expression levels for various experimental animal groups.

3.5. PD-model mice and neuroprotective effects

Fig. 7A and B show neuroprotective effects of treatments on the SN among the various experimental groups. TH staining showed a 60% loss of DA neurons in SN of MPTP mice treated with LpDNA only or with FUS exposure only compared to the control mice. Separate LpDNA/MBs administration following FUS exposure significantly restored TH-positive neurons ($p < 0.05$ compared to other MPTP groups and $p < 0.005$ versus FUS exposure only group). Of note, the administration of LpDNA-MBs following FUS exposure provided the most significant restoration of TH-positive neurons even with a cell count 14% higher than the control group ($p < 0.005$ against MPTP-treated group only and $p < 0.005$ against FUS exposure only group). The reduced number of TH-positive neurons was also consistent with the detected decrease of DA along with its metabolites in the MPTP-treated PD mouse model, as shown in Fig. 6C.

Fig. 7C shows that dopamine active transporter (DAT) expressed in the SN and ST, respectively, as a major band at approximately 24 kDa and that its protein expression in mice treated with LpDNA-MBs plus FUS sonication was greater than other conditions (the normal control, the LpDNA only, and the LpDNA injection followed by avidinylated MBs injection plus FUS exposure). These findings indicate that the use of LpDNA-MBs complex with FUS exposure enhances DA synthesis due to cellular GDNF transduction when compared with LpDNA administration alone ($p < 0.05$) or FUS exposure only ($p < 0.05$). Since DAT level functions in DA re-uptake and the DAT level can reflect the DA metabolism level and function of dopaminergic neuron, the increased DAT

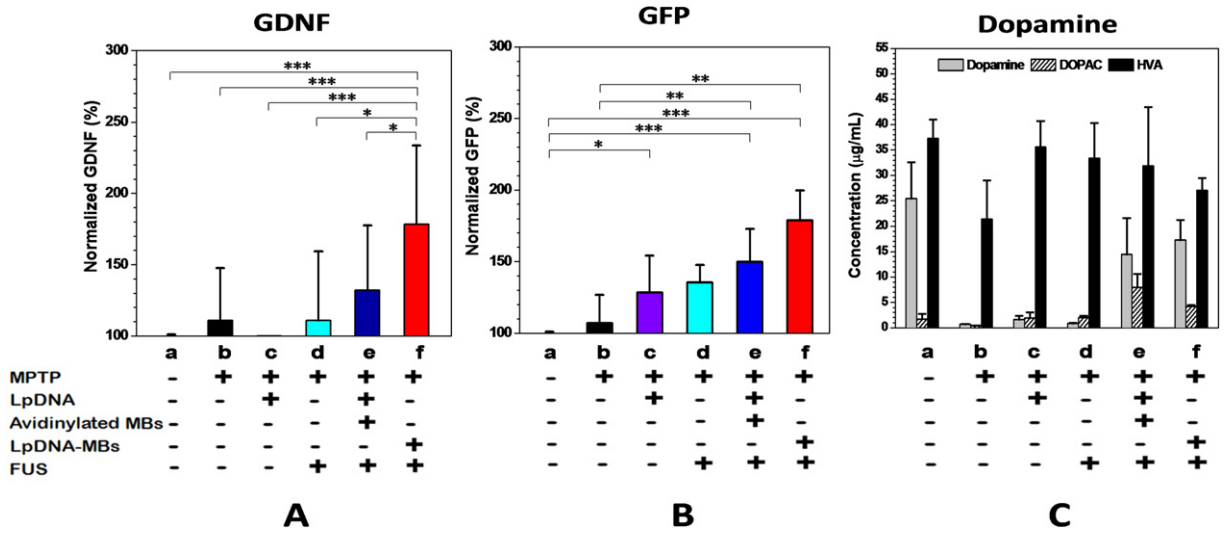

Fig. 6. (A, B) GDNF and GFP expression level quantitated via ELISA immunoassay among various experimental animal groups. (C) Relative concentration levels of dopamine along with its key metabolites, DOPAC and HVA. Statistical analysis for each group was conducted via ANOVA followed by Tukey's post-hoc test. Significant difference was denoted as "*", "**", and "****" to respectively represent $p < 0.05$, $p < 0.01$, and $p < 0.005$.

level confirms the delivery and expression of the GDNF gene into SN of MPTP-mice improved neuronal degeneration.

3.6. Motor-related behavioral recovery after FUS-BBB opening

Fig. 8 shows weekly monitoring results for motor performance among the various experimental groups over a 4-week period. Three-week continuous MPTP injection showed a stable 70% deterioration of home-cage locomotor behavior when compared to the control mice (latency: 9.6 ± 6.1 s versus 36.8 ± 4.3 s in control mice). The LpDNA administration only and FUS exposure groups showed only a slightly improved behavioral deficit but did not reach a significant difference (latency: 23.3 ± 2.4 s versus 18.8 ± 8.5 s in control mice). Separate LpDNA/MBs administration following FUS exposure significantly restored motor related behavioral loss (latency of 40.2 ± 10.3 s). Of note, LpDNA-MBs complex administration following FUS exposure provided the most significant and complete restoration of motor related behavior among different tested groups (latency of 53.7 ± 8.8 s). Behavioral analyses indicated that the LpDNA-MBs complex with FUS exposure provided the most significant improvement of neuronal function.

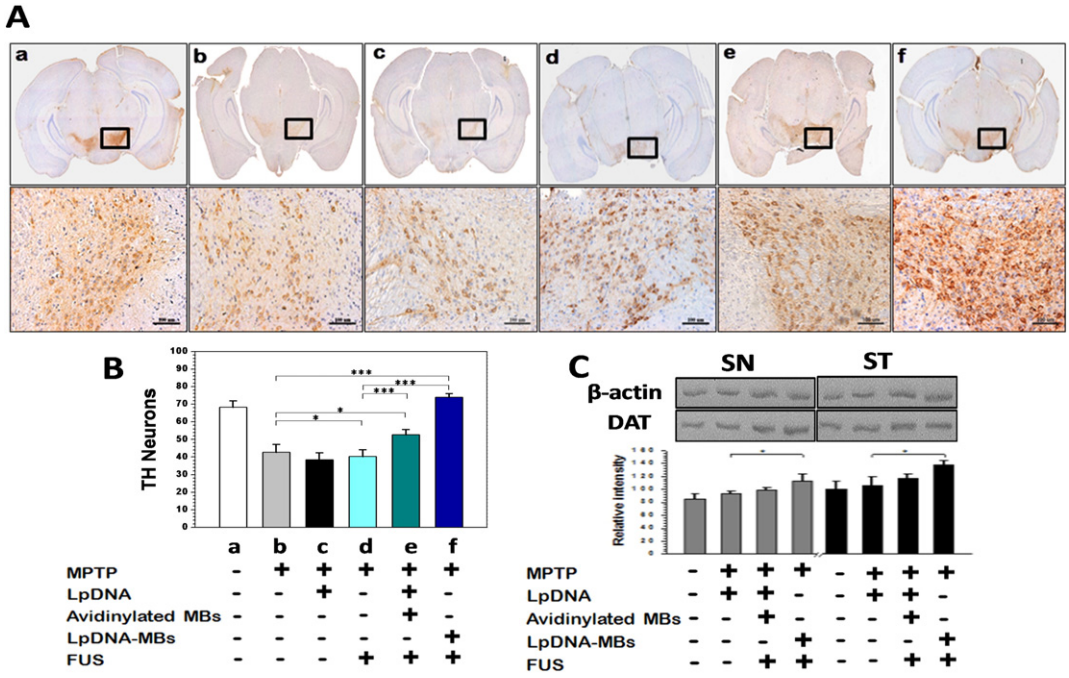

Fig. 7. (A) Immunodetection of Tyrosine hydroxylase (TH)-positive neurons among the various experimental animal groups. Positively-stained sites represent healthy TH neuronal cells (original and ×100 magnifications; scale bar = 100 μm). (B) Number of TH-positive cells in substantia nigra (SN) site among various experimental groups. (C) Dopamine active transporter (DAT) expression at brain SN and striatum (ST) regions among various experimental groups analyzed via Western blot. Blocking at 22 kDa reflects DAT expression, and actin served as a control. Significant difference was denoted as "*" and "**" to respectively represent $p < 0.05$ and $p < 0.005$.

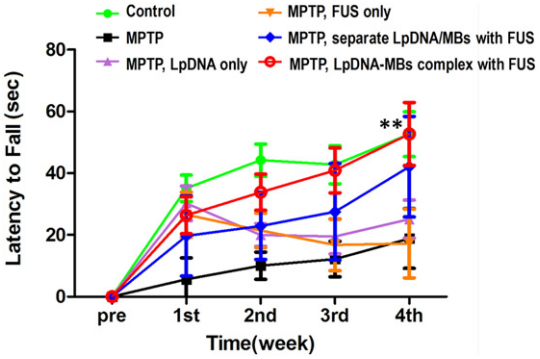

Fig. 8. Motor balance and coordination testing of animal via rotarod test under various experimental groups. Measurements of latency time until fall are from the beam walking test. Data are presented as the mean ± S.D. Significant difference was denoted as "**" to represent $p < 0.01$ via Kolmogorov-Smirnov's tests.

3.7. Immunohistochemistry after FUS-BBB opening

Fig. 9 shows a typical example of immunohistochemically cell staining for GFP and GDNF expression and the correlation with the expressed cell type (Fig. 9A–D: healthy brain control; Fig. 9E–H: PD-model brain control; Fig. 9I–L: PD-model brain treated with LpDNA-MBs plus FUS). Double-labeled IHC (MAP2 to identify neuronal cells and DAPI to mark all cell nuclei) was used to identify gene expressing in neuronal cells (Fig. 9 2nd column). Immunohistochemical detection results show that the proteins GFP and GDNF were expressed in neuronal cells, thus enriching the neural cells around the BBB-opened brain regions via MAP2/DAPI staining (Fig. 9I–J). While the expression levels of GDNF in the neuronal cells were different between the healthy brain control and PD-model brain control, the LpDNA-MBs following FUS exposure showed a significant increase in expression levels, and PD-model brain subjected to this treatment showed the most significant increase of neuronal neurite length and cell count both in terms of GFP and GDNF expression in neuronal cells. (Fig. 9I–J; neurons were identified by their proximal dendrite cell shapes). Of note, many GDNF-positive cells were also GFP-positive, implying that a majority of GDNF-positive cells exhibit neuronal morphology. Overexpressed GDNF proteins from transfected neuronal cells are also likely to be able to stimulate neurite outgrowth and rescue with impaired dopaminergic neurons.

4. Discussion

We previously demonstrated that the systematic encapsulation of plasmid DNA into liposomes (denoted as "LpDNA") can effectively prevent degradation. Concurrent opening of the BBB via FUS exposure allows for the successful delivery of GDNF genes, thus amplifying GDNF expression [22]. This study presents further improvements by conjugating gene-liposomes with microbubbles (MBs) to form gene-liposome-MB complexes (denoted as "LpDNA-MBs") to achieve improved gene delivery efficiency. The proposed system helps restore motor behavioral function increase DA (and its metabolites DOPAC and HVA) secretion/metabolism (indicated by DAT level), and rescue degenerated dopaminergic neuron in the striatum of MPTP-induced mice, an animal model that shows similar symptoms to human PD [6]. Immunohistochemical analysis shows that the GDNF proteins can be overexpressed in the neuronal cells by LpDNA-MBs with the FUS-BBB opening method, suggesting this novel gene delivery system can provide a non-invasive approach for effective CNS gene therapy clinical applications.

In this study, we quantitatively investigated the reporter gene expression in MPTP-induced animal to compare the gene expression efficacy as well as therapeutic efficacy between the proposed LpDNA-MBs complex system and the previously proposed separate administration of LpDNA and MBs. Our results indicate that LpDNA-MBs complex system provided improved targeted gene delivery efficiency. When

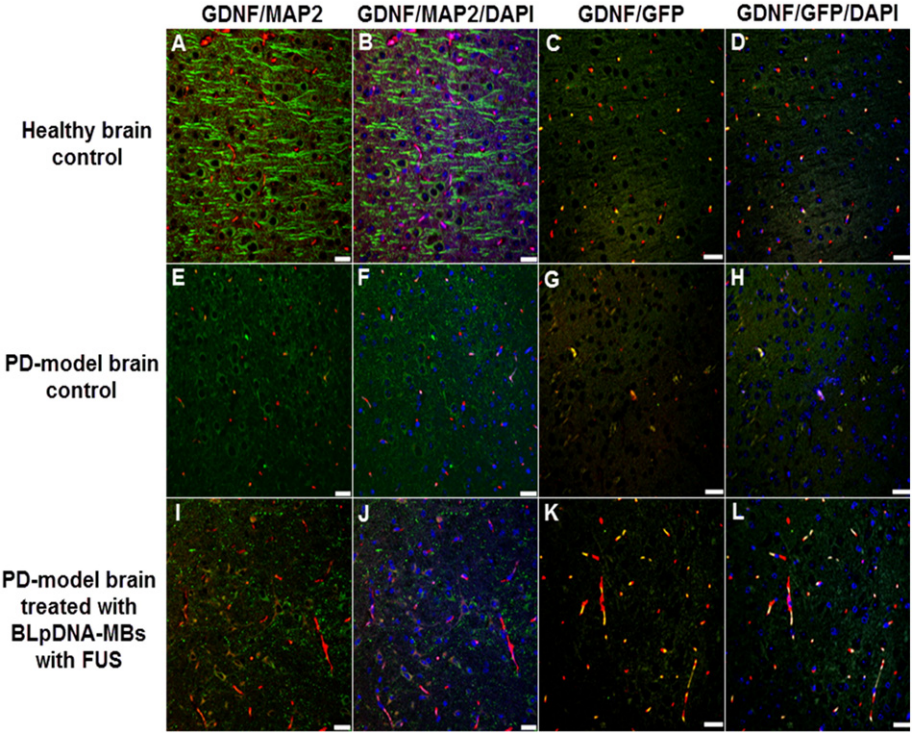

Fig. 9. Immunohistochemistry of in vivo transfection in neuronal cells after gene delivery. Fluorescence staining of brain striatal tissues revealed expression of GDNF and GFP after 4-week interval. Transfected GDNF/MAP2, GDNF/MAP2/DAPI, GDNF/GFP, and GDNF/GFP/DAPI was shown to demonstrate GDNF expression site, GDNF expression site specifically at neuron, as well as colocalized with GFP expression site. Bar = 30 μm. DAPI = 4′,6-diamidino-2-phenylinodole; MAP2 = microtubule-associated proteins (MAPs); GFP = green fluorescence protein; GDNF = glia-derived neurotrophic factor.

microbubble-present FUS exposure at the brain SN, focused ultrasound energy interacts with MBs and triggers bubble vibrations (expansions/contractions) to generate local radial acoustic emissions. The emitted energy causes shear stress in CNS capillary and induces temporal disassembling of tight junction proteins and stimulate active transport [17,18]. This phenomenon in the microvasculature can transiently produce vascular pores and increase of vascular permeability (see Fig. 1), with the simultaneous release of LpDNA near the vascular pores. During MBs oscillation, LpDNA experiences acoustic emissions to allow MBs disconnections, and the radial emissions directs LpDNA toward the disrupted tight-junctional craft and maximize influx-mediated LpDNA transportation into brain parenchyma. This may explain why the LpDNA-MBs complex system with FUS exposure outperforms LpDNA through increased BBB permeability, for the delivery of genes or other therapeutic drugs [22,32,33]. Our results indicate that LpDNA-MB complexes can be use to assist FUS-induced BBB opening to maximize the accumulation of DA, DA's metabolites, GFP, and GDNF in the striatal brain.

LpDNA measuring 200–400 nm in diameter were synthesized for use as a gene vector. During FUS-induced uptake of LpDNA, the ultrasound pressure waves interact with the MBs, causing bubble expansion, followed by bubble growth, oscillation, deformation, and perhaps even stable cavitation. These latter cavitation phenomena may shear and disrupt the LpDNA bilayer membranes or disrupt cell membranes to induce a perforation of the blood vessels and enhance transgene transportation within or into brain cells [34]. Previous studies also supported that cell liposome endocytosis can be triggered and enhanced via ultrasound exposure, therefore supporting enhanced LpDNA uptake [35,36].

We also specially formulated our liposomes to have a positive charge by using DSPE-PEG-(2000)-amine and the positively charged choline groups of DPPC in order to entrap negatively-charged plasmids due to a described previously electrostatic interaction [22]. During liposome synthesis, the hydration of a dry lipid film containing zwitterionic phospholipids and cholesterol with an aqueous suspension of pDNA (a plasmid encoding both the GFP and GDNF genes) was found to constitute stable biotinylated liposomes with slightly positive charges from amine groups of phospholipids. In addition, the positively charged avidinylated MBs and slightly neutral charged biotinylated liposomes were able to conjugate and good transfection activity can be achieved (Fig. 3B). Cryo-TEM images are consistent with our hypothesis that the LpDNAs were conjugated outside the avidinylated MBs by linkage of biotin-avidin (Fig. 3C and D). We also showed that these biotin-avidin linkages are formed primarily between LpDNA and avidinylated MBs to yield a high loading efficiency of pDNA into the LpDNA-MBs complex.

We also showed that the proposed system effectively enhanced neurotrophic factor synthesis in the brain and provides improved neuroprotective effects for impaired neuronal cells (Figs. 7 and 8). TH-positive neurons, dopamine active transporter (DAT), and motor performance were significantly improved through the concurrent administration of LpDNA-MBs complexes with FUS exposure. Without MBs, FUS exposure alone and LpDNA injection alone did not induce such an improvement since the gene-vector cannot penetrate the BBB, thus supporting the need to open the BBB via FUS exposure for the systematic delivery of genes into the CNS.

To investigate GDNF expression level and DA secretion/activity/metabolism, animals were sacrificed postoperatively to evaluate neuroprotective efficacy for biochemical analysis including quantitative analysis of DA level, its metabolites DOPAC and HVA, GDNF, and GFP, as well as DAT. We showed that the LpDNA-MBs complex system with FUS exposure indeed promoted cellular transfection and transduction in the nucleus, and promoted DA expression in the SN of brain, thus restoring motor function of MPTP-treated animals. Some studies have demonstrated that the neuroprotective action by large amount of GDNF on the nigrostriatal system might also involve the activation of protein kinase [37,38] or induce nuclear factor pathways to promote neuronal survival from toxic insults [29,39]. Hence, this study may serve as a starting point to further study of mechanisms involved in the proposed gene-delivering system.

Other investigators have also presented MB-carrier vesicles designed for drug delivery [40]. Our previous study also demonstrated a similar strategy in conjugating a gene vector with MBs to promote gene delivery and improve neuroprotective efficacy [41]. In these previous reports, liposome/MBs with a cationic charge were synthesized to increase the loading efficacy. In addition, perfluorocarbon (PFC) gas was used in MBs, with the gas core typically formulated to form a vapor phase. In this study, LpDNA-MBs formulation was not only distinct in the lipid composition but also in the synthesis procedure. We loaded pDNA into biotinylated liposomes by zwitterionic phospholipids with positively charged amino groups to create a neutral formulation in order to maintain systemic circulation over a prolonged period of time. A potential benefit of the proposed synthesis approach is to increase the complex's gene-vector payload and potentially prolong circulation time during intravenous administration.

5. Conclusion

This study demonstrated that GDNF genes can be delivered into CNS dopaminergic neurons via the concurrent administration of gene-vector-MBs complexes and noninvasive and targeted FUS-induced BBB opening. We have shown that the gene-vector-MBs complexes were superior to separate gene-vector/MBs administration in terms of GDNF/GFP gene delivery to the SN of brain. We also confirmed successful GDNF transduction in dopaminergic neurons to recover normal secretion of DA (and metabolites), along with a neuroprotective effect and the restoration of PD-model motor behavior. These results suggest that the proposed CNS gene delivery system has potential as a therapeutic strategy for neurodegenerative diseases such as PD and Alzheimer's and Huntington's disease.

Acknowledgements

This work was supported by the Ministry of Science and Technology, Taiwan, under grants nos. 101-2221-E-182-002-MY3 and 102-2221-E-182-020-MY3, and by Chang Gung Memorial Hospital, Taiwan, under grants nos. CIRPD2E0051, CMRPD2D0111-3, CMRPD2A0031-3, CLRPG3D0012, and CIRPD3E0131-3. The MRI imaging studies were carried out with the help of the Center of Advanced Molecular Imaging and Translation, Chang Gung Memorial Hospital, Linkou, Taiwan. We also thank the Microscope Core Laboratory, Chang Gung Memorial Hospital, Linkou for their assistance in the experiment.

References

[1] N. Pankratz, T. Foroud, Genetics of Parkinson disease, Genet. Med. 9 (2007) 801–811.
[2] H. Braak, E. Braak, D. Yilmazer, C. Schultz, R.A. de Vos, E.N. Jansen, Nigral and extranigral pathology in Parkinson's disease, J. Neural Transm. Suppl. 46 (1995) 15–31.
[3] S.K. Van Den Eeden, C.M. Tanner, A.L. Bernstein, R.D. Fross, A. Leimpeter, D.A. Bloch, L.M. Nelson, Incidence of Parkinson's disease: variation by age, gender, and race/ethnicity, Am. J. Epidemiol. 157 (2003) 1015–1022.
[4] M.T. Brown, P. Henny, J.P. Bolam, P.J. Magill, Activity of neurochemically heterogeneous dopaminergic neurons in the substantia nigra during spontaneous and driven changes in brain state, J. Neurosci. 29 (2009) 2915–2925.
[5] K.M. Costa, The effects of aging on substantia nigra dopamine neurons, J. Neurosci. 34 (2014) 15133–15134.
[6] P.G. Coune, B.L. Schneider, P. Aebischer, Parkinson's disease: gene therapies, Cold Spring Harb. Perspect. Med. 2 (2012) a009431.
[7] A. Siderowf, M.B. Stern, Premotor Parkinson's disease: clinical features, detection, and prospects for treatment, Ann. Neurol. 64 (Suppl. 2) (2008) S139–S147.
[8] R.E. Burke, GDNF as a candidate striatal target-derived neurotrophic factor for the development of substantia nigra dopamine neurons, J. Neural Transm. Suppl. 70 (2006) 41–45.
[9] D.M. Gash, Z. Zhang, A. Ovadia, W.A. Cass, A. Yi, L. Simmerman, D. Russell, D. Martin, P.A. Lapchak, F. Collins, B.J. Hoffer, G.A. Gerhardt, Functional recovery in parkinsonian monkeys treated with GDNF, Nature 380 (1996) 252–255.
[10] J.H. Kordower, M.E. Emborg, J. Bloch, S.Y. Ma, Y. Chu, L. Leventhal, J. McBride, E.Y. Chen, S. Palfi, B.Z. Roitberg, W.D. Brown, J.E. Holden, R. Pyzalski, M.D. Taylor, P.

Carvey, Z. Ling, D. Trono, P. Hantraye, N. Deglon, P. Aebischer, Neurodegeneration prevented by lentiviral vector delivery of GDNF in primate models of Parkinson's disease, Science 290 (2000) 767–773.
[11] A.D. Zurn, H.R. Widmer, P. Aebischer, Sustained delivery of GDNF: towards a treatment for Parkinson's disease, Brain Res. Brain Res. Rev. 36 (2001) 222–229.
[12] H.L. Liu, C.Y. Huang, J.Y. Chen, H.Y. Wang, P.Y. Chen, K.C. Wei, Pharmacodynamic and therapeutic investigation of focused ultrasound-induced blood-brain barrier opening for enhanced temozolomide delivery in glioma treatment, PLoS One 9 (2014), e114311.
[13] Y. Takakura, M. Nishikawa, F. Yamashita, M. Hashida, Development of gene drug delivery systems based on pharmacokinetic studies, Eur. J. Pharm. Sci. 13 (2001) 71–76.
[14] J.G. Nutt, K.J. Burchiel, C.L. Comella, J. Jankovic, A.E. Lang, E.R. Laws Jr., A.M. Lozano, R.D. Penn, R.K. Simpson Jr., M. Stacy, G.F. Wooten, Randomized, double-blind trial of glial cell line-derived neurotrophic factor (GDNF) in PD, Neurology 60 (2003) 69–73.
[15] W.Y. Chai, P.C. Chu, M.Y. Tsai, Y.C. Lin, J.J. Wang, K.C. Wei, Y.Y. Wai, H.L. Liu, Magnetic-resonance imaging for kinetic analysis of permeability changes during focused ultrasound-induced blood-brain barrier opening and brain drug delivery, J. Control. Release 192 (2014) 1–9.
[16] P.Y. Chen, H.Y. Hsieh, C.Y. Huang, C.Y. Lin, K.C. Wei, H.L. Liu, Focused ultrasound-induced blood-brain barrier opening to enhance interleukin-12 delivery for brain tumor immunotherapy: a preclinical feasibility study, J. Transl. Med. 13 (2015) 93.
[17] K. Hynynen, N. McDannold, N.A. Sheikov, F.A. Jolesz, N. Vykhodtseva, Local and reversible blood–brain barrier disruption by noninvasive focused ultrasound at frequencies suitable for trans-skull sonications, NeuroImage 24 (2005) 12–20.
[18] K. Hynynen, N. McDannold, N. Vykhodtseva, F.A. Jolesz, Noninvasive MR imaging–guided focal opening of the blood-brain barrier in rabbits, Radiology 220 (2001) 640–646.
[19] H.L. Liu, M.Y. Hua, P.Y. Chen, P.C. Chu, C.H. Pan, H.W. Yang, C.Y. Huang, J.J. Wang, T.C. Yen, K.C. Wei, Blood-brain barrier disruption with focused ultrasound enhances delivery of chemotherapeutic drugs for glioblastoma treatment, Radiology 255 (2010) 415–425.
[20] H.L. Liu, M.Y. Hua, H.W. Yang, C.Y. Huang, P.C. Chu, J.S. Wu, I.C. Tseng, J.J. Wang, T.C. Yen, P.Y. Chen, K.C. Wei, Magnetic resonance monitoring of focused ultrasound/magnetic nanoparticle targeting delivery of therapeutic agents to the brain, Proc. Natl. Acad. Sci. U. S. A. 107 (2010) 15205–15210.
[21] K.C. Wei, H.C. Tsai, Y.J. Lu, H.W. Yang, M.Y. Hua, M.F. Wu, P.Y. Chen, C.Y. Huang, T.C. Yen, H.L. Liu, Neuronavigation-guided focused ultrasound-induced blood-brain barrier opening: a preliminary study in swine, AJNR Am. J. Neuroradiol. 34 (2013) 115–120.
[22] C.Y. Lin, H.Y. Hsieh, W.G. Pitt, C.Y. Huang, I.C. Tseng, C.K. Yeh, K.C. Wei, H.L. Liu, Focused ultrasound-induced blood-brain barrier opening for non-viral, non-invasive, and targeted gene delivery, J. Control. Release 212 (2015) 1–9.
[23] R.M. Richardson, A.P. Kells, K.H. Rosenbluth, E.A. Salegio, M.S. Fiandaca, P.S. Larson, P.A. Starr, A.J. Martin, R.R. Lonser, H.J. Federoff, J.R. Forsayeth, K.S. Bankiewicz, Interventional MRI-guided putaminal delivery of AAV2-GDNF for a planned clinical trial in Parkinson's disease, Mol. Ther. 19 (2011) 1048–1057.
[24] E. Garbayo, C.N. Montero-Menei, E. Ansorena, J.L. Lanciego, M.S. Aymerich, M.J. Blanco-Prieto, Effective GDNF brain delivery using microspheres—a promising strategy for Parkinson's disease, J. Control. Release 135 (2009) 119–126.
[25] A.L. Klibanov, T.I. Shevchenko, B.I. Raju, R. Seip, C.T. Chin, Ultrasound-triggered release of materials entrapped in microbubble-liposome constructs: a tool for targeted drug delivery, J. Control. Release 148 (2010) 13–17.
[26] F. Yan, L. Li, Z. Deng, Q. Jin, J. Chen, W. Yang, C.K. Yeh, J. Wu, R. Shandas, X. Liu, H. Zheng, Paclitaxel-liposome-microbubble complexes as ultrasound-triggered therapeutic drug delivery carriers, J. Control. Release 166 (2013) 246–255.
[27] C.Y. Lin, M. Javadi, D.M. Belnap, J.R. Barrow, W.G. Pitt, Ultrasound sensitive eLiposomes containing doxorubicin for drug targeting therapy, Nanomed. Nanotechnol. Biol. Med. 10 (2014) 67–76.
[28] V. Jackson-Lewis, S. Przedborski, Protocol for the MPTP mouse model of Parkinson's disease, Nat. Protoc. 2 (2007) 141–151.
[29] Z. Guo, S. Xu, N. Du, J. Liu, Y. Huang, M. Han, Neuroprotective effects of stemazole in the MPTP-induced acute model of Parkinson's disease: involvement of the dopamine system, Neurosci. Lett. 616 (2016) 152–159.
[30] R.S. Burns, Subclinical damage to the nigrostriatal dopamine system by MPTP as a model of preclinical Parkinson's disease: a review, Acta Neurol. Scand. Suppl. 136 (1991) 29–36.
[31] M.M. Bradford, A rapid and sensitive method for the quantitation of microgram quantities of protein utilizing the principle of protein-dye binding, Anal. Biochem. 72 (1976) 248–254.
[32] A. Burgess, S. Dubey, S. Yeung, O. Hough, N. Eterman, I. Aubert, K. Hynynen, Alzheimer disease in a mouse model: MR imaging-guided focused ultrasound targeted to the hippocampus opens the blood-brain barrier and improves pathologic abnormalities and behavior, Radiology 273 (2014) 736–745.
[33] T. Nhan, A. Burgess, E.E. Cho, B. Stefanovic, L. Lilge, K. Hynynen, Drug delivery to the brain by focused ultrasound induced blood-brain barrier disruption: quantitative evaluation of enhanced permeability of cerebral vasculature using two-photon microscopy, J. Control. Release 172 (2013) 274–280.
[34] B.P. Mead, P. Mastorakos, J.S. Suk, A.L. Klibanov, J. Hanes, R.J. Price, Targeted gene transfer to the brain via the delivery of brain-penetrating DNA nanoparticles with focused ultrasound, J. Control. Release 223 (2016) 109–117.
[35] S. Koch, P. Pohl, U. Cobet, N.G. Rainov, Ultrasound enhancement of liposome-mediated cell transfection is caused by cavitation effects, Ultrasound Med. Biol. 26 (2000) 897–903.
[36] R. Suzuki, T. Takizawa, Y. Negishi, K. Hagisawa, K. Tanaka, K. Sawamura, N. Utoguchi, T. Nishioka, K. Maruyama, Gene delivery by combination of novel liposomal bubbles with perfluoropropane and ultrasound, J. Control. Release 117 (2007) 130–136.
[37] C.C. Chao, C.H. Chiang, Y.L. Ma, E.H. Lee, Molecular mechanism of the neurotrophic effect of GDNF on DA neurons: role of protein kinase CK2, Neurobiol. Aging 27 (2006) 105–118.
[38] X. d'Anglemont de Tassigny, A. Pascual, J. Lopez-Barneo, GDNF-based therapies, GDNF-producing interneurons, and trophic support of the dopaminergic nigrostriatal pathway. Implications for Parkinson's disease, Front. Neuroanat. 9 (2015) 10.
[39] J.P. Cao, H.J. Wang, J.K. Yu, H.M. Liu, D.S. Gao, The involvement of NF-kappaB p65/p52 in the effects of GDNF on DA neurons in early PD rats, Brain Res. Bull. 76 (2008) 505–511.
[40] I. Lentacker, N. Wang, R.E. Vandenbroucke, J. Demeester, S.C. De Smedt, N.N. Sanders, Ultrasound exposure of lipoplex loaded microbubbles facilitates direct cytoplasmic entry of the lipoplexes, Mol. Pharm. 6 (2009) 457–467.
[41] C.H. Fan, C.Y. Ting, C.Y. Lin, H.L. Chan, Y.C. Chang, Y.Y. Chen, H.L. Liu, C.K. Yeh, Noninvasive, targeted, and non-viral ultrasound-mediated GDNF-plasmid delivery for treatment of Parkinson's disease, Sci. Rep. 6 (2016) 19579.